

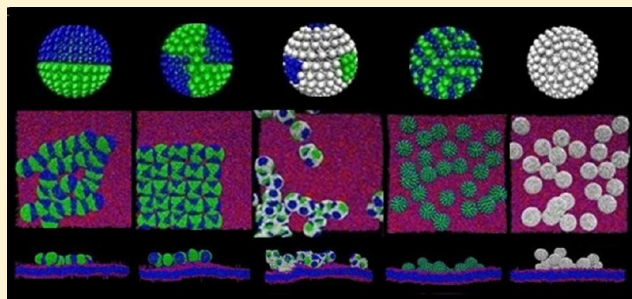
Self-Assembly of Patterned Nanoparticles on Cellular Membranes: Effect of Charge Distribution

Ye Li, Xianren Zhang,* and Dapeng Cao*

Division of Molecular and Materials Simulation, State Key Laboratory of Organic–Inorganic Composites, Beijing University of Chemical Technology, Beijing 100029, People's Republic of China

ABSTRACT: Nanoparticle-assisted drug delivery has been emerging as an active research area. Achieving high drug loading is only one facet of drug delivery issues; it is also important to investigate the effect of surface charge distribution on self-assembly of nanoparticles on cellular membranes. By considering the electrostatic distribution of patterned nanoparticles, we used dissipative particle dynamics simulations to investigate the self-assembly of pattern charged nanoparticles with five different surface charged patterns. It is found that both surface charged pattern and nanoparticle size significantly affect the self-assembly of nanoparticles on cellular membranes.

Results indicate that 1/2 pattern charged small nanoparticles can self-assemble into dendritic structures, while those with a 1/4 pattern self-assemble into clusters. As the nanoparticle size increases, 1/2 pattern charged medium nanoparticles can self-assemble into linear structures, while those with a 1/4 pattern self-assemble into clusters. For very large nanoparticles, both 1/2 pattern and 1/4 pattern charged nanoparticles self-assemble into flaky structures with different connections. By considering the effects of surface charged pattern and nanoparticle size on self-assembly, we found that nanoparticle self-assembly requires a minimum effective charged area. When the local charged area of nanoparticles is less than the threshold, surface charge cannot induce nanoparticle self-assembly; that is, the surface charged pattern of a nanoparticle would determine effectively the self-assembly structure. It is expected that this work will provide guidance for nanoparticle-assisted drug delivery.



INTRODUCTION

Self-assembly plays a very important role in many aspects in both nature and nanotechnology,¹ such as protein^{2,3} and DNA^{4–7} self-assembly in biological systems, synthesis of porous templates by block copolymers⁸, and the self-assembly related to smart materials.⁹ There are also many examples of functionalizing the surface of nanoparticles with DNA oligonucleotides, genetically engineered proteins, and antibody/antigen pairs.^{10–12} The complementarity of these biomolecules provides a specificity that has been used to direct the self-assembly of nanoparticles into aggregates by changing temperature, solvent pH, salt concentration, and other variables. At the same time, future materials and devices for photonics, electronics, drug delivery systems, and sensors require the self-assembly of synthetic nanostructures with the precision and reliability of biological self-assembly.

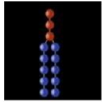

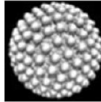
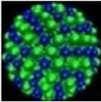
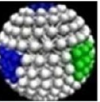
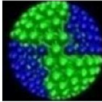
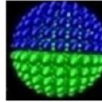
Lately, nanoparticles are receiving much attention because they can act as carriers and be used to translocate proteins, drug molecules, and other useful matter into cells, which has very promising applications in drug/gene delivery. Previous investigations indicate that the distribution of organic molecules within the stabilizer coating is anisotropic and inhomogeneous^{13–18} and the nanoparticles can spontaneously assemble into highly ordered structures. For example, Kotov et al. observed the spontaneous formation of wires, chains, and sheets in suspensions of thiol-coated CdTe nanoparticles and attributed this behavior to inhomogeneous patchiness in the

coating.^{13,17,18} Additionally, the geometry of small particles, which deviates significantly from a generic spherical shape, can induce orientation-specific interactions at a nanometer scale.¹⁹ It has been argued that an exceptionally large dipole moment, arising apparently from the nearly tetrahedral shape of small CdSe or CdTe nanoparticles in water, induces their self-assemblies into chains and rings^{18,20–22} reminiscent of certain assembled protein structures.²³ Glozer et al. observed that chain, sheet, ring, icosahedral, square pyramid, tetrahedral, twisted, and staircase structures can be obtained by suitably designing the surface pattern of the patches represented by the attractive interaction sites.²⁴ In addition, Granick et al. have observed the self-assembly of spherical particles with opposite electric charges on both hemispheres into clusters that were formed in aqueous suspension.²⁴ Previous studies of self-assembly were mainly focused on three-dimensional space.^{24,25} In a two-dimensional membrane surface, Cacciuto et al. found that lipid membranes can mediate linear aggregation of spherical nanoparticles, binding them for a wide range of biologically relevant bending rigidities.²⁶ Actually, in previous theoretical studies, few works considered the effects of the charge on the nanoparticle self-assembly.²⁵ However, in a realistic biological system, almost all proteins, viruses, and

Received: December 10, 2012

Revised: May 6, 2013

Table 1. Nanoparticles with Different Surface Charged Patterns^a

Model							
Type	lipid	Structure	Uncharged NP	Random NP	Patchy NP	1/4 NP	1/2 NP

^aNanoparticle core is shown in white. Positively charged ligands are shown in green and negatively charged ligands in dark blue. Specific region is shown in yellow and hydrophilic region in red.

nanoparticles are charged, and they always interact with the cellular membrane. Hayden et al. experimentally observed the aggregation and interaction of cationic nanoparticles on bacterial surfaces²⁷ and matrix protein self-assembly.²⁸ The surface properties of the nanoparticle also play an important role in the interaction of a nanoparticle and a membrane. For example, Stellacci et al. compared the membrane penetration behavior of two nanoparticle “isomers” with similar composition, where one is coated with subnanometer striations of alternating anionic and hydrophobic groups and the other is coated with the same moieties but in a random distribution, and found that the former penetrates the plasma membrane without bilayer disruption, whereas the latter is mostly trapped in endosomes.²⁹ Apparently, these interactions are linked with the charge distribution on the surface of the nanoparticles. Therefore, it is important to investigate the effects of nanoparticle surface charge distribution on self-assembly on a membrane. Here, we construct a charged nanoparticle/cell membrane model to investigate the self-assembly of charged nanoparticles on a cellular membrane to further explore the effect of charge distribution on nanoparticle self-assembly.

In this work, by introducing electrostatic interactions into dissipative particle dynamics (DPD) simulations, we investigated the self-assemblies of different pattern charged nanoparticles on biological membranes and further examined the effects of nanoparticle surface charge distribution on the formation of different structures. Finally, we also discuss the potential application of this system design to drug/gene delivery.

MODELS AND SIMULATION METHODS

In this work, DPD simulations were performed to investigate the self-assembly of charged patterned nanoparticles on cellular membranes. The DPD method has been used to simulate the hydrodynamic behavior of complex fluids^{30–32} in which the dynamics of DPD beads are governed by Newton’s equation of motion, similar to molecular dynamics (MD). The DPD method has become one of the most commonly used computer simulation techniques to study biomembrane systems,^{33–43} including the interactions between biomembranes and nanoparticles,^{35,38,41,44} because it can accurately reproduce the dynamic behavior of a lipid bilayer.

Here, a coarse-grained model was used to represent different patterned nanoparticles. A schematic diagram of the system is given in Table 1. The hydrophilic portion (N_h) of the nanoparticle is shown in red in Table 1. In addition, the nanoparticles also have a small specific portion (N_t) at the terminus which is shown in yellow in Table 1. The yellow surface segments have specific interactions with lipid head groups, which make nanoparticles adhere to the membrane. The small specific portion is approximately proportional to the nanoparticle size. To represent dimyristoylphosphatidylcholine (DMPC), a lipid molecule⁴⁵ is modeled by connecting a

headgroup with three hydrophilic beads (H) to two hydrophobic tails of equal length, each having five hydrophobic beads (T), shown in Table 1. A water molecule is represented by a single bead (W).

The interaction force exerted on a bead is composed of conservative, dissipative, and random forces. The conservative force between beads i and j , which is soft and repulsive, is determined by

$$F_{ij}^C = a_{ij} \hat{r}_{ij} \max \left\{ 1 - \frac{r_{ij}}{r_c}, 0 \right\} \quad (1)$$

where a_{ij} is the maximum repulsive force between particles i and j , $r_{ij} = r_j - r_i$ (r_i and r_j are the positions of particles i and j , respectively), $r_{ij} = |r_{ij}|$, $\hat{r}_{ij} = r_{ij}/|r_{ij}|$, and r_c is the cutoff radius. In this system, the interaction parameters between the same species beads were set to $a_{TT} = a_{WW} = a_{HH} = 25$, suggesting that the same species have a weak attraction. Those between different species were $a_{HW} = 25$, $a_{TW} = 80$, $a_{HT} = 50$, $a_{N_hH} = a_{N_tW} = 25$, $a_{N_hT} = a_{N_tW} = 80$, $a_{N_hH} = 5$, and $a_{N_hW} = 20$.

In the model of lipid molecules, the interaction between neighboring beads within the same molecule is described by a harmonic spring force, given by

$$F_S = K_S(r_{ij} - r_{eq})\hat{r}_{ij} \quad (2)$$

where the spring constant, K_S , was set to $128k_B T$ and the equilibrium bond length, r_{eq} , was set to $0.7r_c$. The force constraining the variation of bond angle is given by

$$F_\phi = -\nabla U_\phi \text{ and } U_\phi = K_\phi(1 - \cos(\phi - \phi_0)) \quad (3)$$

where ϕ_0 was set to π and K_ϕ is the bond bending constant equal to 10.0 for lipid molecules.

Generally, we selected the interaction cutoff radius r_c , bead mass m , and thermostat temperature $k_B T$ to be unity in the simulations. To relate r_c to its actual physical size, we used the formula proposed by Groot and Rabone,⁴⁶ $r_c = 3.107(\rho N_m)^{1/3}$ (Å). Here, N_m was set to 3, ρ was set to 3.0, and a water molecule has an approximate volume of 30 Å^3 . Accordingly, we obtained $r_c = 6.46 \text{ Å}$.

In the DPD simulations, the electrostatic interactions among the charged particles were solved by coupling all the particles to a local electrostatic field, which was solved on a lattice and updated by^{47–49}

$$\psi^{\text{new}} = \psi^{\text{old}} + \frac{d\Psi}{dt} \quad (4)$$

with

$$\frac{d\psi(r)}{dt} = \xi[\Gamma \bar{\rho}_e(r) + \nabla \cdot (P(r) \nabla \psi)] \quad (5)$$

Here $\xi = 0.15$ is the analog of a friction factor. $\Gamma = e^2/k_B T \epsilon_0 \epsilon_r r_0$ = 9.615 is a coupling constant at room temperature that is

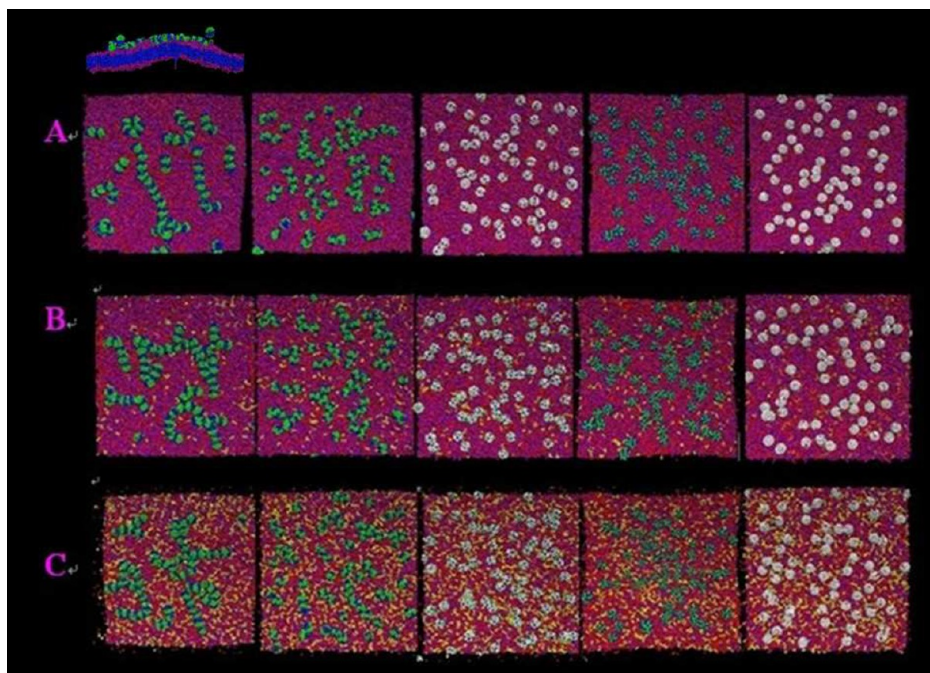


Figure 1. Typical snapshots of nanoparticle self-assembly after 240 ns. Nanoparticle cores are shown in white, positively charged ligands in green, negatively charged ligands in dark blue, negatively charged lipid heads in yellow, neutral lipid heads in purple, and lipid tails in dark blue. A side view of 1/2 pattern nanoparticles on the uncharged membrane is shown above row A. In the simulations, the nanoparticle diameter was set to 3.23 nm. (A) The negatively charged lipid to neutral lipid ratio is 0/10. (B) The negatively charged lipid to neutral lipid ratio is 1/10. (C) The negatively charged lipid to neutral lipid ratio is 7/10. (In A, B, and C from left to right: 1/2 pattern charged nanoparticle, 1/4 pattern charged nanoparticle, patch pattern charged nanoparticle, random pattern charged nanoparticle, and uncharged nanoparticle.)

independent of position. ϵ_0 is the dielectric constant for a vacuum, and ϵ_r is the relative permittivity of water at room temperature. The dielectric permittivity $\epsilon = \epsilon_0 \epsilon_r(r)$ is extracted by defining a permittivity relative to the value in pure water, namely $\epsilon = \epsilon_0 \epsilon_r p(r)$. Here the dielectric constant of a vacuum ϵ_0 was set to $8.85418782 \times 10^{-12} \text{ C}^2 \text{ J}^{-1} \text{ m}^{-1}$, and $\epsilon_r = 78.3$ is adopted from the relative permittivity of water at 25 °C. $p(r) = \langle p_i \rangle_{\text{cell}}$ is the polarizability relative to pure water, where the average $\langle \dots \rangle_{\text{cell}}$ runs over all particles in a cell around r . p_i is the polarizability of particle i ; $p = 1$ for water, and $p \approx 0.025$ for hydrocarbons.⁴⁸ $\bar{\rho}_e$ is the averaged local charged density, which is defined by

$$\bar{\rho}_e(r) = \int f(|r - r'|) \rho_e(r') d^3r' \quad (6)$$

The charge distribution function is given by

$$f(r) = \frac{3}{\pi R_e^3} \left(1 - \frac{r}{R_e} \right), \text{ for } r < R_e \quad (7)$$

and $f(r) = 0$ for $r > R_e$. Here, $R_e = 1.6r_0$ and is the electrostatic smearing radius. The validity of this method was verified using the standard Ewald sum approach⁵⁰ for the bulk electrolyte– and polyelectrolyte–surfactant solutions.

In this work, we used an N-varied DPD method that is a particular variant of the DPD method in which the targeted membrane tension is maintained by monitoring the number of lipids per area (LNPA) in a boundary region^{38,39,44} to simulate the internalization processes. In this method, the boundary region, which surrounds the central square region of the membrane, plays a role as a reservoir of lipids, and the value of LNPA in the boundary region (denoted as $\rho_{\text{LNPA}}^{\text{BR}}$) is kept constant by deletion/addition moves. Simultaneously, a

corresponding number of water beads is randomly deleted or added to keep the whole density of the simulation box constant.

To investigate the effect of the surface pattern on nanoparticle self-assembly, five types of nanoparticles with various charged patterns were designed: (1) uncharged, (2) 1/2 pattern of alternating positive and negative charges, (3) 1/4 pattern of alternating positive and negative charges, (4) patch charged pattern, and (5) randomly charged pattern mixed with the same positive and negative charge ratios (Table 1). The charged ligands coated on the surface of nanoparticles have a net charge of $-e$. Each nanoparticle is neutral because the positive and negative charges on each nanoparticle are equal. The negatively charged lipid membrane was achieved by making the first head bead of some lipids carry a net charge of $-e$. The counterion is a single bead carrying one positive charge.

RESULTS AND DISCUSSION

We mainly investigated the self-assembly of charged nanoparticles on a lipid membrane. The focus was placed on the effects of surface charged pattern, size of the nanoparticles, and electric quantity of the negatively charged lipid membrane on the nanoparticle self-assembly. To consider the effect of nanoparticle size on self-assembly, we explored three types of nanoparticles with diameters of 3.23, 4.5, and 7.1 nm. We labeled the 3.23 nm nanoparticles as small, the 4.5 nm nanoparticles as medium, and the 7.1 nm nanoparticles as large.

First, we put the small nanoparticles into an 8×8 matrix structure on the membrane surface. After 240 ns, we found that the 1/2 pattern charged small nanoparticles self-assembled into dendritic structures and a few partial ringlike structures, while the 1/4 pattern charged small nanoparticles self-assembled into clusters, as shown in the first two snapshots in Figure 1A.

However, the other pattern charged nanoparticles do not show obvious aggregates (see the last three snapshots in Figure 1A). We used three methods to further characterize the aggregation degree of nanoparticles. First, we present in Figure 2 the

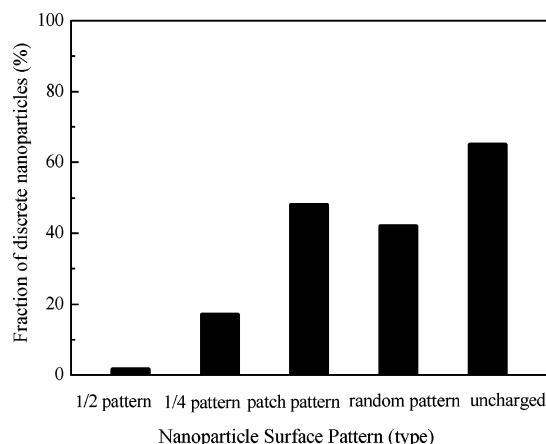


Figure 2. The fraction of discrete nanoparticle number ($D = 3.23$ nm) with the uncharged membrane.

discrete degree of the different pattern charged nanoparticles on the neutral lipid membrane. When the nanoparticles do not contact other ones, we marked it as “discrete”. The discrete degree of the 1/2 pattern charged nanoparticles is 1.6%, but it is 17% for 1/4 pattern charged nanoparticles, 42% for patch pattern charged nanoparticles, 48% for random pattern charged nanoparticles, and 65% for uncharged nanoparticles. With the decrease of the locally charged area of nanoparticles, the discrete degree of the nanoparticles increases, suggesting that nanoparticle aggregation needs a minimum effective charged area. When the surface charged area of the nanoparticles is smaller than the minimum effective charged threshold, the nanoparticles show good dispersion without aggregation. For the nanoparticle designed for drug/gene delivery, its aggregation structure plays a very important role in the internalization process. Previous investigations indicate that it is quite difficult for single, small nanodrug particles to enter the cell by means of endocytosis^{51–54} because it costs more bending energy to be packaged by a lipid membrane. Instead, the small nanoparticles generally cluster into a closely packed aggregate on the membrane and then achieve the internalization process.⁵⁵ Accordingly, for nanoparticles designed for drug delivery, the 1/4 charged pattern is suitable for this purpose because it is easy to form a cluster, benefiting endocytosis. If the small nanoparticles organize into linear aggregates, they can promote the formation of membrane tubes,^{56,57} which do not benefit nanoparticle endocytosis.

According to statistics about the maximum cluster size of different pattern charged nanoparticles on the neutral lipid membrane (Figure 3), it is found that the maximum cluster size is 16 for 1/2 pattern charged nanoparticles, 10 for 1/4 pattern charged nanoparticles, 4 for patch pattern charged nanoparticles, 7 for random pattern charged nanoparticles, and 4 for uncharged nanoparticles. With the decrease of the locally charged area of the nanoparticles, the maximum cluster size decreases. This is the reason why the patch pattern charged, random pattern charged, and uncharged nanoparticles do not show obvious aggregate structures. In addition, we present the average cluster size of the different pattern charged nano-

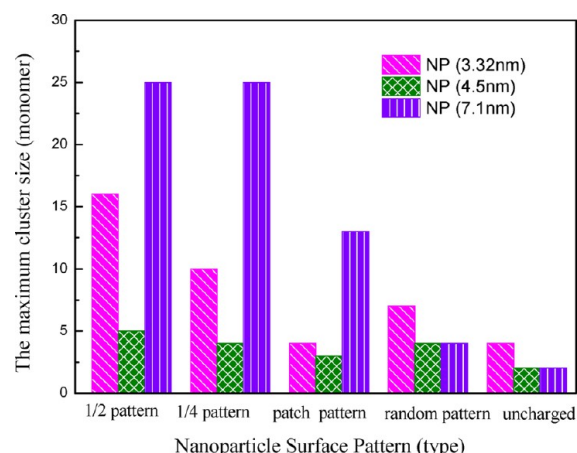


Figure 3. The maximum cluster size of different pattern charged nanoparticles on the uncharged membrane.

particles in Figure 4. With a decrease of the locally charged area of the nanoparticles, the average cluster size also decreases.

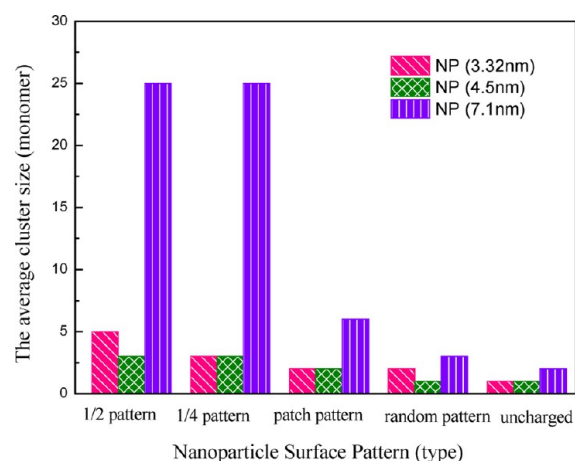


Figure 4. The average cluster size of different pattern charged nanoparticles on the uncharged membrane.

In practical cell research, the cellular membrane is often charged. Accordingly, we considered the effect of membrane charge on nanoparticle self-assembly and explored these cases for the different patterned nanoparticles on a negatively charged membrane. Rows B and C of Figure 1 show snapshots of different patterned nanoparticles on the partially charged lipid membranes in which randomly selected 1/10 lipids and 2/5 lipids were negatively charged. According to the statistics about the discrete degree of different patterned nanoparticles on different lipid membranes (see Table 2), it is found that nanoparticle self-assembly does not exhibit a significant difference for the charged versus uncharged membranes, as shown in rows B and C of Figure 1. This means that the charge distribution of the nanoparticles is more dominant than the membrane charge for nanoparticle self-assembly.

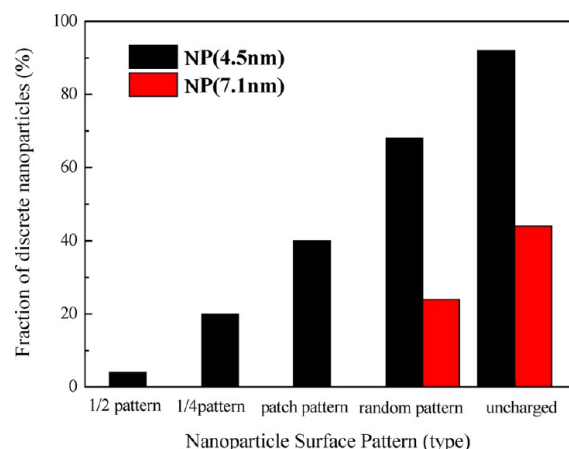
In order to further research the influence of nanoparticle size on nanoparticle self-assembly, we also simulated the medium nanoparticle system with a 5×5 matrix structure on the membrane. Within 240 ns, 1/2 pattern charged nanoparticles self-assemble into short chain structures, while 1/4 pattern charged nanoparticles self-assemble into small clusters, as shown in the first two snapshots in Figure 5A. The small

Table 2. The Number of Discrete Nanoparticles with Different Surface Charge Patterns on Different Lipid Membranes^a

nanoparticle ^c	uncharged ^b			1/10 charged ^c			7/10 charged ^d		
	a	b	c	a	b	c	a	b	c
uncharged	1	1	0	1	3	0	1	3	0
randomly charged	11	5	0	7	1	0	22	4	1
patch charged	31	10	0	28	8	2	34	4	0
1/4 charged	27	17	6	27	15	11	26	13	8
1/2 charged	42	23	11	31	17	6	40	21	13

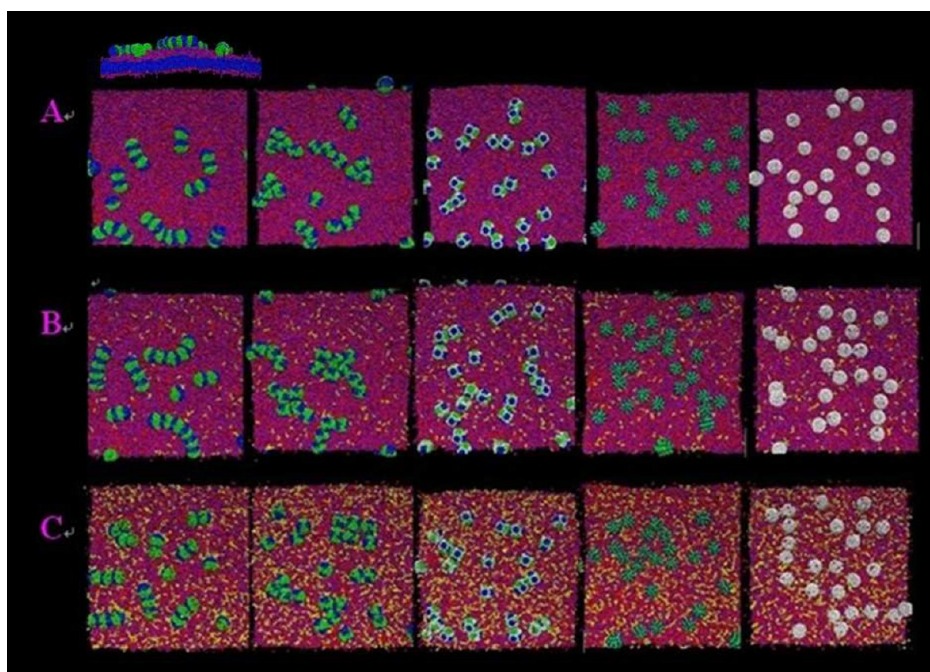
^aDiscrete indicates that nanoparticles do not assemble into aggregates. ^bMembrane is uncharged. ^cOne of ten lipids on the membrane is negatively charged. ^dSeven of ten lipids on the membrane are negatively charged. ^eNanoparticle diameters: a, 3.23 nm; b, 4.5 nm; c, 7.1 nm.

aggregates appear for the patch pattern charged nanoparticle, while it is absent for the small nanoparticles presented earlier. The randomly patterned charged and the uncharged nanoparticles do not show aggregates yet, as shown in the last two snapshots in Figure 5A. It is found that the nanoparticle discrete degree increases linearly with the decrease of nanoparticle surface charged area (Figure 6). Both the maximum and the average cluster size decrease with the decrease of nanoparticle surface charged area (see Figures 3 and 4). This also suggests that the locally charged area of nanoparticles is a key factor determining self-assembly. When the charged area is larger than a certain effective area, the nanoparticle self-assembly happens easily. Similar to the case of

**Figure 6.** The fraction of discrete nanoparticle number ($D = 4.5$ nm, $D = 7.1$ nm) with the uncharged membrane.

small particles, the membrane charge does not show a significant effect on nanoparticle self-assembly (see Table 2).

Interestingly, the 1/2 pattern and 1/4 pattern charged large nanoparticles self-assemble into flaky structures with different connections. As mentioned above, the 1/2 pattern charged small nanoparticles form dendritic structures (Figure 1A), while the 1/2 pattern charged medium nanoparticles self-assemble into short lines (Figure 5A). For the 1/2 pattern charged large nanoparticles, the formed chains would further connect together to yield a flaky structure. The reason may be that with the increase in nanoparticle size, the excess effective charge area in large nanoparticles can connect the chains together. Similarly, 1/4 pattern charged large nanoparticles also form the

**Figure 5.** Typical snapshots of nanoparticle self-assembly after 240 ns. Nanoparticle cores are shown in white, positively charged ligands in green, negatively charged ligands in dark blue, negatively charged lipid heads in yellow, neutral lipid heads in purple, and lipid tails in dark blue. The side view of 1/2 pattern nanoparticles on the uncharged membrane is shown above row A. In the simulations, the nanoparticle diameter was set to 4.5 nm. (A) The negatively charged lipid to neutral lipid ratio is 0/10. (B) The negatively charged lipid to neutral lipid ratio is 1/10. (C) The negatively charged lipid to neutral lipid ratio is 7/10. (In A, B, and C from left to right: 1/2 pattern charged nanoparticles, 1/4 pattern charged nanoparticles, patch pattern charged nanoparticles, random pattern charged nanoparticles, and uncharged nanoparticles.)

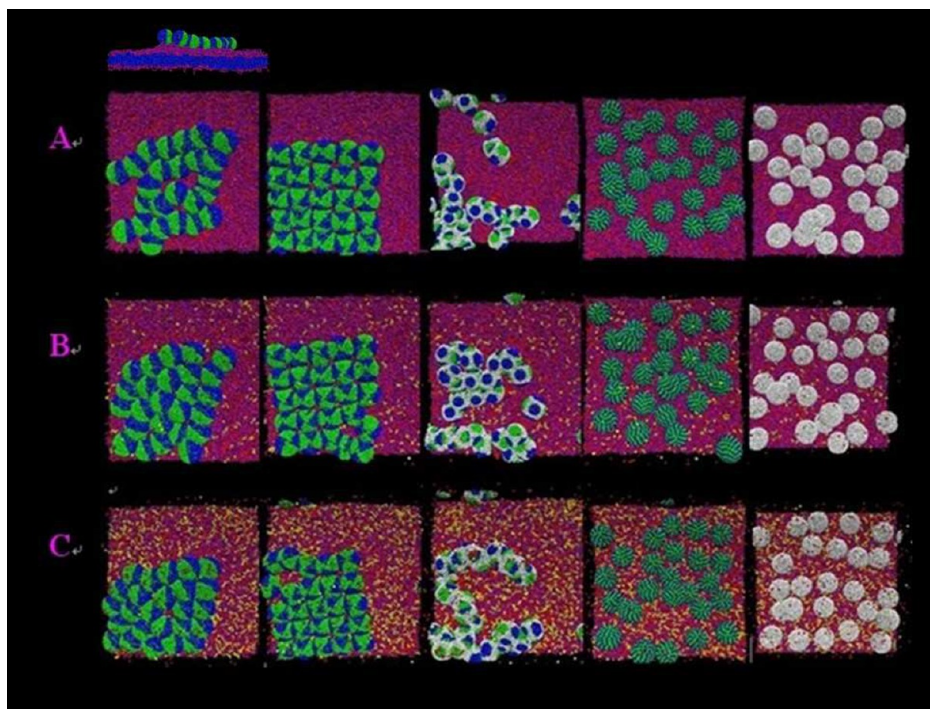


Figure 7. Typical snapshots of nanoparticle self-assembly after 240 ns. Nanoparticle cores are shown in white, positively charged ligands in green, negatively charged ligands in dark blue, negatively charged lipid heads in yellow, neutral lipid heads in purple, and lipid tails in dark blue. A side view of 1/2 pattern nanoparticles on the uncharged membrane is shown above row A. In the simulations, the nanoparticle diameter was set to 7.1 nm. (A) The negatively charged lipid to neutral lipid ratio is 0/10. (B) The negatively charged lipid to neutral lipid ratio is 1/10. (C) The negatively charged lipid to neutral lipids ratio is 7/10. (In A, B, and C from left to right: 1/2 pattern charged nanoparticles, 1/4 pattern charged nanoparticles, patch pattern charged nanoparticles, random pattern charged nanoparticles, and uncharged nanoparticles.)

flaky structure (see Figure 7A). The patch pattern charged large nanoparticles self-assemble into chain or cluster structures (Figure 7A), which are absent in the case of small nanoparticles. The discrete degree, maximum cluster size, and average cluster size of large nanoparticles exhibit behaviors similar to those of medium nanoparticles. It is noted that the flaky structure formed by the 1/2 and 1/4 charged pattern large nanoparticles would affect the order of the lipid and induce local gelation.⁵⁸ In our simulations, no wrapping of the nanoparticles by the membranes was observed, which is different from the penetration behavior of stripy nanoparticles into a lipid membrane.²⁹

In general, salt always exists in a real biological cell. In order to explore the effect of salt on nanoparticle self-assembly on the membrane, we selected the case of 1/4 pattern nanoparticles on the uncharged membrane as an example. Figure 8 shows typical top view (top row) and side view (bottom row) snapshots of self-assembly of different size nanoparticles on the uncharged membrane in the presence of salt, where the salt content is 0.09%. Although salt was considered in the case, the self-assembled structures of nanoparticles do not show significant difference from the case without salt. Both the maximum and the average clusters exhibit only a slight decrease for 4.5 and 3.23 nm nanoparticles in the presence of salt, as shown in Figures 9 and 10. This means the salt only slightly decreases the aggregate degree of charged nanoparticles, especially for the smaller ones.

Actually, this work provides a qualitative understanding of the fact that normal proteins can disperse very well in an organism to keep it active and realize its normal physiological activities. The charge on a protein surface is relatively scattered,

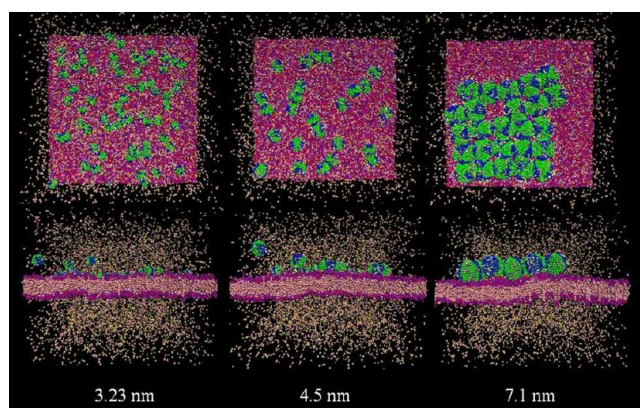


Figure 8. Typical snapshots of nanoparticles with different sizes self-assembling on uncharged membrane in the presence of salt after 240 ns. Top view (top row), side view (bottom row) snapshots of self-assembly of different size nanoparticles on the uncharged membrane in the presence of salt, where the salt content is 0.09%. Although salt was considered in the case, the self-assembled structures of nanoparticles do not show significant difference from the case without salt. Both the maximum and the average clusters exhibit only a slight decrease for 4.5 and 3.23 nm nanoparticles in the presence of salt, as shown in Figures 9 and 10. This means the salt only slightly decreases the aggregate degree of charged nanoparticles, especially for the smaller ones.

which does not lead to excessive gathering and inactivation, whereas a gene mutation often leads to excessive aggregation associated with neurodegenerative diseases.^{59–61}

CONCLUSIONS

We have used DPD simulations to investigate the self-assembly of pattern charged nanoparticles on cellular membranes. It is found that the nanoparticle self-assembly needs a minimum effective charged area. When the local charged area of

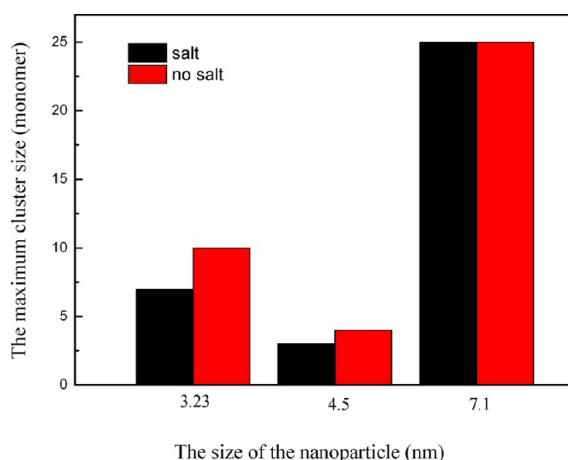


Figure 9. The maximum cluster size for 1/4 pattern charged nanoparticles of different sizes on the uncharged membrane.

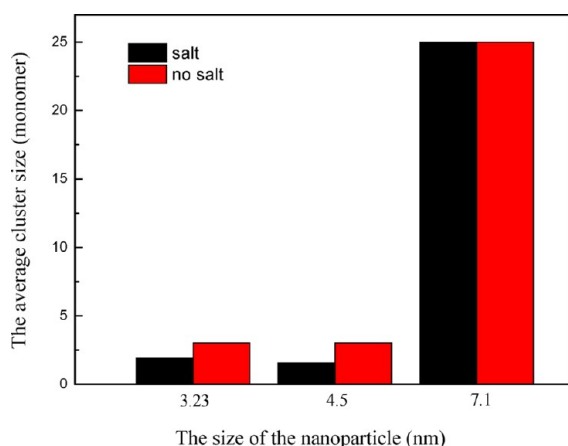


Figure 10. The average cluster size for 1/4 pattern charged nanoparticles of different sizes on the uncharged membrane.

nanoparticles is less than the threshold, its surface charge cannot induce nanoparticle self-assembly; that is, the surface charge pattern of nanoparticles would determine effectively the self-assembly structure. In addition, nanoparticle size is also a very important factor affecting nanoparticle self-assembly structures. For a small nanoparticle designed for drug delivery, we believe that a 1/4 charge pattern is suitable because it can form clusters, benefiting its endocytosis and accelerating drug delivery. In addition, we also investigated the effects of the membrane charge on the charged nanoparticle self-assembly, and results indicated that the membrane charge does not show a significant effect on nanoparticle self-assembly. Similarly, the presence of salt only slightly decreases the aggregate degree, especially for the small nanoparticles. Actually, this work can provide a reasonable explanation for the fact that some charged viruses and proteins can self-assemble into different structures on a biological membrane: these charged viruses and proteins possess different surface charge patterns. It is also expected that this work can give a reference for the design of nanoparticles as drug/gene delivery, which can effectively control the nanoparticle self-assembly structure by tailoring nanoparticle size and surface charge pattern.

AUTHOR INFORMATION

Corresponding Author

*E-mail: X.Z., zhangxr@mail.buct.edu.cn; D.C., caodp@mail.buct.edu.cn.

Notes

The authors declare no competing financial interest.

ACKNOWLEDGMENTS

This work is supported by National 973 Program (2011CB706900), NSF of China (21274011, 21276007), and Chemical Grid Program and Excellent Talent of BUCT. The authors thank Dr. Lianghui Gao from Beijing Normal University for fruitful discussions.

REFERENCES

- (1) Whitesides, G. M.; Grzybowski, B. Self-Assembly at all Scales. *Science* **2002**, *295*, 2418–2421.
- (2) Ou, W. C.; Wang, M.; Fung, C.; Tsai, R.; Chao, P.; Hseu, T.; Chang, D. The Major Capsid Protein, VP1, of Human JC Virus Expressed in *Escherichia coli* is able to Self-assemble into a Capsid-Like Particle and Deliver Exogenous DNA into Human Kidney Cells. *J. Gen. Virol.* **1999**, *80*, 39–46.
- (3) Kimbaurer, R.; Booy, F.; Cheng, N.; Lowy, D.; Schiller, J. Papillomavirus L1 Major Capsid Protein Self-Assembles into Virus-Like Particles that are Highly Immunogenic. *Proc. Natl. Acad. Sci. U.S.A.* **1992**, *89*, 12180–12184.
- (4) Cai, L.; Tabata, H.; Kawai, T. Self-Assembled DNA Networks and Their Electrical Conductivity. *Appl. Phys. Lett.* **2000**, *77*, 3105–3106.
- (5) Winfree, E.; Liu, F.; Wenzler, L. A.; Seeman, N. C. Design and Self-Assembly of Two-Dimensional DNA Crystals. *Nature* **1998**, *394*, 539–544.
- (6) He, Y.; Chen, Y.; Liu, H.; Ribbe, A. E.; Mao, C. Self-Assembly of Hexagonal DNA Two-Dimensional (2D) Arrays. *J. Am. Chem. Soc.* **2005**, *127*, 12202–12203.
- (7) He, Y.; Ye, T.; Su, M.; Zhang, C.; Ribbe, A. E.; Jiang, W.; Mao, C. Hierarchical Self-Assembly of DNA into Symmetric Supramolecular Polyhedra. *Nature* **2008**, *452*, 198–201.
- (8) Cheng, L.; Cao, D. Self-Assembly of Star-Polymer-Attached Nanospheres for Polymer Nanocomposites. *J. Phys. Chem. C* **2010**, *114*, 5732–5740.
- (9) Cheng, L.; Cao, D. Designing a Thermo-switchable Channel for Nanofluidic Controllable Transportation. *ACS Nano* **2011**, *5*, 1102–1108.
- (10) Parak, W. J.; Gerion, D.; Pellegrino, T.; Zanchet, D.; Micheel, C.; Williams, S. C.; Boudreau, R.; Le Gros, M. A.; Larabell, C. A.; Alivisatos, A. P. Biological Applications of Colloidal Nanocrystals. *Nanotechnology* **2003**, *14*, R15–R27.
- (11) Banerjee, I. A.; Yu, L.; Matsui, H. Location-Specific Biological Functionalization on Nanotubes: Attachment of Proteins at the Ends of Nanotubes Using Au Nanocrystal Masks. *Nano Lett.* **2003**, *3*, 283–287.
- (12) Mirkin, C. A.; Letsinger, R. L.; Mucic, R. C.; Storhoff, J. J. A DNA-Based Method for Rationally Assembling Nanoparticles into Macroscopic Materials. *Nature* **1996**, *382*, 607–609.
- (13) Wang, Y.; Tang, Z.; Liang, X.; Liz-Marzán, L. M.; Kotov, N. A. SiO₂-coated CdTe Nanowires: Bristled Nano Centipedes. *Nano Lett.* **2004**, *4*, 225–231.
- (14) Li, F.; Ding, Y.; Gao, P.; Xin, X.; Wang, Z. L. Single-Crystal Hexagonal Disks and Rings of ZnO: Low-Temperature, Large-Scale Synthesis and Growth Mechanism. *Angew. Chem., Int. Ed.* **2004**, *43*, 5238–5242.
- (15) Punter, V. F.; Krishnan, K. M.; Alivisatos, A. P. Colloidal Nanocrystal Shape and Size Control: The Case of Cobalt. *Science* **2001**, *291*, 2115–2117.

- (16) Peng, X.; Manna, L.; Yang, W.; Wickham, J.; Scher, E.; Kadavanich, A.; Alivisatos, A. Shape Control of CdSe Nanocrystals. *Nature* **2000**, *404*, 59–61.
- (17) Ahmadi, T. S.; Wang, Z. L.; Green, T. C.; Henglein, A.; El-Sayed, M. A. Shape-Controlled Synthesis of Colloidal Platinum Nanoparticles. *Science* **1996**, *272*, 1924–1925.
- (18) Tang, Z.; Kotov, N. A.; Giersig, M. Spontaneous Organization of Single CdTe Nanoparticles into Luminescent Nanowires. *Science* **2002**, *297*, 237–240.
- (19) Wang, Z. L.; Harfenist, S. A.; Vezmar, I.; Whetten, R. L.; Bentley, J.; Evans, N. D.; Alexander, K. B. Superlattices of Self-Assembled Tetrahedral Ag Nanocrystals. *Adv. Mater. (Weinheim, Ger.)* **1998**, *10*, 808–812.
- (20) Li, L. S.; Alivisatos, A. P. Origin and Scaling of the Permanent Dipole Moment in CdSe Nanorods. *Phys. Rev. Lett.* **2003**, *90*, 97402–97406.
- (21) Shim, M.; Guyot-Sionnest, P. Permanent Dipole Moment and Charges in Colloidal Semiconductor Quantum Dots. *J. Chem. Phys.* **1999**, *111*, 6955–6965.
- (22) Rabani, E. Structure and Electrostatic Properties of Passivated CdSe Nanocrystals. *J. Chem. Phys.* **2001**, *115*, 1493.
- (23) Kavanagh, G. M.; Clark, A. H.; Ross-Murphy, S. B. Heat-Induced Gelation of Globular Proteins: Part 3. Molecular Studies on Low pH β -lactoglobulin Gels. *Int. J. Biol. Macromol.* **2000**, *28*, 41–50.
- (24) Zhang, Z.; Glotzer, S. C. Self-Assembly of Patchy Particles. *Nano Lett.* **2004**, *4*, 1407–1413.
- (25) Hong, L.; Cacciuto, A.; Luijten, E.; Granick, S. Clusters of Charged Janus Spheres. *Nano Lett.* **2006**, *6*, 2510–2514.
- (26) Šarić, A.; Cacciuto, A. Fluid Membranes Can Drive Linear Aggregation of Adsorbed Spherical Nanoparticles. *Phys. Rev. Lett.* **2012**, *108*, 118101–118106.
- (27) Hayden, S. C.; Zhao, G.; Saha, K.; Phillips, R. L.; Li, X.; Miranda, O. R.; Rotello, V. M.; El-Sayed, M. A.; Schmidt-Krey, I.; Bunz, U. H. F. Aggregation and Interaction of Cationic Nanoparticles on Bacterial Surfaces. *J. Am. Chem. Soc.* **2012**, *134*, 6920–6923.
- (28) Chen, C. L.; Bromley, K. M.; Moradian-Oldak, J.; DeYoreo, J. J. In Situ AFM Study of Amelogenin Assembly and Disassembly Dynamics on Charged Surfaces Provides Insights on Matrix Protein Self-Assembly. *J. Am. Chem. Soc.* **2011**, *133*, 17406–17413.
- (29) Verma, A.; Uzun, O.; Hu, Y.; Hu, Y.; Han, H.-S.; Watson, N.; Chen, S.; Irvine, D. J.; Stellacci, F. Surface-Structure-Regulated Cell-Membrane Penetration by Monolayer-Protected Nanoparticles. *Nat. Mater.* **2008**, *7*, 588–595.
- (30) Groot, R. D.; Warren, P. B. Dissipative Particle Dynamics: Bridging the Gap Between Atomistic and Mesoscopic Simulation. *J. Chem. Phys.* **1997**, *107*, 4423–4435.
- (31) Hoogerbrugge, P. J.; Koelman, J. Simulating Microscopic Hydrodynamic Phenomena with Dissipative Particle Dynamics. *Europhys. Lett.* **1992**, *19*, 155–160.
- (32) Espanol, P.; Warren, P. Statistical Mechanics of Dissipative Particle Dynamics. *Europhys. Lett.* **1995**, *30*, 191–196.
- (33) Li, S.; Zhang, X.; Wang, W. Cluster Formation of Anchored Proteins Induced by Membrane-Mediated Interaction. *Biophys. J.* **2010**, *98*, 2554–2563.
- (34) Li, S.; Zhang, X.; Wang, W. Coarse-Grained Model for Mechanosensitive Ion Channels. *J. Phys. Chem. B* **2009**, *113*, 14431–14438.
- (35) Yang, K.; Ma, Y. Computer Simulation of the Translocation of Nanoparticles with Different Shapes Across a Lipid Bilayer. *Nanotechnol.* **2010**, *5*, 578–583.
- (36) Laradji, M.; Sunil Kumar, P. B. Dynamics of Domain Growth in Self-Assembled Fluid Vesicles. *Phys. Rev. Lett.* **2004**, *93*, 198105.
- (37) Alexeev, A.; Uspal, W. E.; Balazs, A. C. Harnessing Janus Nanoparticles to Create Controllable Pores in Membranes. *ACS Nano* **2008**, *2*, 1117–1122.
- (38) Yue, T.; Zhang, X. Molecular Understanding of Receptor-Mediated Membrane Responses to Ligand-Coated Nanoparticles. *Soft Matter* **2011**, *7*, 9140–9112.
- (39) Yue, T.; Li, S.; Zhang, X.; Wang, W. The Relationship between Membrane Curvature Generation and Clustering of Anchored Proteins: A Computer Simulation Study. *Soft Matter* **2010**, *6*, 6109–6118.
- (40) Venturoli, M.; Smit, B.; Sperotto, M. M. Simulation Studies of Protein-Induced Bilayer Deformations, and Lipid-Induced Protein Tilting, on a Mesoscopic Model for Lipid Bilayers with Embedded Proteins. *Biophys. J.* **2005**, *88*, 1778–1798.
- (41) Shillcock, J. C.; Lipowsky, R. Tension-Induced Fusion of Bilayer Membranes and Vesicles. *Nat. Mater.* **2005**, *4*, 225–228.
- (42) Gao, L.; Lipowsky, R.; Shillcock, J. Tension-Induced Vesicle Fusion: Pathways and Pore Dynamics. *Soft Matter* **2008**, *4*, 1208–1214.
- (43) Smith, K. A.; Jasnow, D.; Balazs, A. C. Designing Synthetic Vesicles that Engulf Nanoscopic Particles. *J. Chem. Phys.* **2007**, *127*, 084703–084713.
- (44) Li, Y.; Yue, T.; Yang, K.; Zhang, X. Molecular Modeling of the Relationship Between Nanoparticle Shape Anisotropy and Endocytosis Kinetics. *Biomaterials* **2012**, *33*, 4965–4973.
- (45) De Meyer, F. J. M.; Venturoli, M.; Smit, B. Molecular Simulation of Lipid-Mediated Protein-Protein Interactions. *Biophys. J.* **2008**, *95*, 1851–1865.
- (46) Groot, R. D.; Rabone, K. L. Mesoscopic Simulation of Cell Membrane Damage, Morphology Change and Rupture by Nonionic Surfactants. *Biophys. J.* **2001**, *81*, 725–736.
- (47) Gao, L.; Fang, W. Effects of Induced Tension and Electrostatic Interactions on the Mechanisms of Antimicrobial Peptide Translocation across Lipid Bilayer. *Soft Matter* **2009**, *5*, 3312–3318.
- (48) Groot, R. D. Electrostatic Interactions in Dissipative Particle Dynamics—Simulation of Polyelectrolytes and Anionic Surfactants. *J. Chem. Phys.* **2003**, *118*, 11265–11278.
- (49) Gao, L.; Cao, J.; Fang, W. Self-Assembly of Lamellar Lipid–DNA Complexes Simulated by Explicit Solvent Counterion Model. *J. Phys. Chem. B* **2010**, *114*, 7261–7264.
- (50) González-Melchor, M.; Mayoral, E.; Velázquez, M. E.; Alejandre, J. Electrostatic Interactions in Dissipative Particle Dynamics Using the Ewald Sums. *J. Chem. Phys.* **2006**, *125*, 224107–224116.
- (51) Yue, T.; Zhang, X. Molecular Understanding of Receptor-Mediated Membrane Responses to Ligand-Coated Nanoparticles. *Soft Matter* **2011**, *7*, 9104–9112.
- (52) Zhang, S.; Li, J.; Lykotrafitis, G.; Bao, G.; Suresh, S. Size-Dependent Endocytosis of Nanoparticles. *Adv. Mater. (Weinheim, Ger.)* **2008**, *21*, 419–424.
- (53) Gao, H.; Shi, W.; Freund, L. B. Mechanics of Receptor-Mediated Endocytosis. *Proc. Natl. Acad. Sci. U.S.A.* **2005**, *102*, 9469–9474.
- (54) Desai, M. P.; Labhasetwar, V.; Walter, E.; Levy, R. J.; Amidon, G. L. The Mechanism of Uptake of Biodegradable Microparticles in Caco-2 Cells is Size Dependent. *Pharm. Res.* **1997**, *14*, 1568–1573.
- (55) Yue, T.; Zhang, X. Cooperative Effect in Receptor-Mediated Endocytosis of Multiple Nanoparticles. *ACS Nano* **2012**, *6*, 3196–3205.
- (56) Bahrami, A. H.; Lipowsky, R.; Weikl, T. R. Tubulation and Aggregation of Spherical Nanoparticles Adsorbed on Vesicles. *Phys. Rev. Lett.* **2012**, *109*, 188102.
- (57) Saric, A.; Cacciuto, A. Mechanism of Membrane Tube Formation Induced by Adhesive Nanocomponents. *Phys. Rev. Lett.* **2012**, *109*, 188101.
- (58) Wang, B.; Zhang, L.; Bae, S. C.; Granick, S. Nanoparticle-Induced Surface Reconstruction of Phospholipid Membranes. *Proc. Natl. Acad. Sci. U.S.A.* **2008**, *105*, 18171–18175.
- (59) Ross, C. A.; Poirier, M. A. Protein Aggregation and Neurodegenerative Disease. *Nat. Med.* **2004**, *10*, s10–s17.
- (60) Koo, E. H.; Lansbury, P. T., Jr.; Kelly, J. W. Amyloid Diseases: Abnormal Protein Aggregation in Neurodegeneration. *Proc. Natl. Acad. Sci. U.S.A.* **1999**, *96*, 9989–9990.
- (61) Shastri, B. S. Neurodegenerative Disorders of Protein Aggregation. *Neurochem. Int.* **2003**, *43*, 1–7.